RSC Advances

ROYAL SOCIETY OF CHEMISTRY

www.rsc.org/advances

Cite this: DOI: 10.1039/c0xx00000x

www.rsc.org/xxxxxx

COMMUNICATION

Nanofibrous silicon/carbon composite sheet derived from cellulose substance as free-standing lithium-ion battery anodes†

Mengya Wang, Dongling Jia, Jiao Li and Jianguo Huang*

Received (in XXX, XXX) Xth XXXXXXXXX 20XX, Accepted Xth XXXXXXXXX 20XX

DOI: 10.1039/b000000x

Free-standing silicon/carbon composites composed of carbon nanofibres coated with a thin silicon layer consisting of fine silicon nanocrystals were fabricated employing cellulose substance (*e.g.*, filter paper) as both structural scaffolds and carbon source, which were used as self-supporting anodes for Li-ion batteries showing good areal capacity, improved cycling stability and excellent rate capability.

The recent decades have witnessed the rapid and significant progresses in the development of rechargeable lithium-ion batteries aiming at powering the various portable electronic devices with high energy densities and long cycle lives. The related electrode materials play the key role in the battery performances, quite a number of attempts have been made to develop next-generation anode materials to replace the traditionally used graphite due to its low specific capacity (372 mAh g^{-1}); and among which, silicon is one of the most promising candidates because of the high theoretical capacity (*ca.* 4200 mAh g^{-1}), low discharge potential and safety.[1] However, the application of silicon powders as anodes in the batteries is limited resulting from the low intrinsic electric conductivity and rapid capacity decay caused by the large volume change upon lithium insertion and extraction processes. To address these challenges, nanostructured silicon materials with varied fine structures have been fabricated and tested as anode materials by taking advantage of their ability to relax strain, such as silicon nanoparticles and the hybrid composited with silicon nanowires,[2] three-dimensional porous silicon particles and nanoporous silicon networks,[3] silicon nanowires[4] and nanotubes,[5] as well as silicon hollow nanospheres.[6]

On the other hand, it is an ideal strategy to employ the silicon/carbon composite matters as anode materials, where the carbon components act as a structural buffer to improve the stability of the anodes; moreover, the good electrical conductivity and long cycle life of the carbon phase contribute to better electrochemical performances of the batteries. Carbon coated silicon nanoparticles with core-shell structures were fabricated by hydrothermal carbonization or *in situ* polymerization processes and were applied as anode materials;[7] silicon nanoparticles were encapsulated inside carbon spheres or tubes giving the composite anode materials to mitigate the pulverization problem of the silicon component.[8] Besides, various silicon/carbon composite nanofibres were prepared by electrospinning and subsequent carbonization processes[9] or by chemical vapour deposition technique[10] achieving enhanced anode stabilities; and graphen-warpped silicon nanowires were recently fabricated by an electrostatic self-assembly process showing improved rate capability and cycling performance.[11] One of the notable advances in the state-of-the-art development of silicon/carbon composite matters for anodes of Li-ion batteries is that a number of such composites have been synthesized and employed as the working electrodes without adding any polymer binder or conducting additive. To this end, silicon/carbon composite nanofibres,[12] free-standing composite films composed of carbon nanotubes (or nanofibres) and silicon nanoparticles (or nanowires),[13] silicon/carbon composite fabrics and textiles,[14] silicon/carbon-nanotube composite papers and sponge,[15] as well as silicon/carbon nanocables sandwiched between reduced graphene oxide sheets[16] have been fabricated to improve the anode performances. However, it still remains a challenge to achieve highly stable capacity retention upon long range cycling.

Herein we report the fabrication of a unique hierarchically structured nanofibrous silicon/carbon composite sheet derived from natural cellulose substance (*e.g.*, ordinary laboratory quantitative filter paper), which was used directly as self-supporting binder-free anodes for Li-ion batteries, enhanced areal capacity, capacity retention and rate performance were achieved owing to the three-dimensional porous network structures of the composite that inherited from the cellulose substance which acted as both structural scaffold and carbon source. It has been proven that biomimetic synthesis is an effective pathway to synthesize artificial functional materials with designed properties.[17] We pioneered the replication of the macro- to nano-structures of natural cellulose substances with metal oxides to give functional nanomaterials,[18] and the approach developed has been demonstrated to be a facile, versatile and efficient methodology for the fabrication of various three-dimensional nanoarchitectures with specific functionalities.[19]

The fabrication process of the nanofibrous silicon/carbon composite sheet is illustrated in Scheme S1 (ESI†). Ultrathin silica gel films were firstly deposited to coat each nanofibre of the filter paper by means of a surface sol–gel process using

Department of Chemistry, Zhejiang University, Hangzhou, Zhejiang 310027, China. E-mail: jghuang@zju.edu.cn; Fax: +86 571 8795 1202

† Electronic supplementary information (ESI) available: Experimental details; electron micrographs, XPS and XRD spectra of the related samples. See DOI: 10.1039/b000000x/

tetramethoxysilane as precursor (Scheme S1b, ESI†).[19e] The as-deposited silica/cellulose composite sheet was subjected to carbonization at 600 °C under argon atmosphere giving the silica/carbon composite sheet (Scheme S1c, ESI†), which was composed of carbon nanofibres coated with thin amorphous silica layer, possessing the corresponding structural hierarchies of the initial filter paper (Fig. S1, ESI†). The silica component of the silica/carbon composite sheet was reduced to silicon by gaseous magnesium at 750 °C for 3 h in argon atmosphere employing a home-made stainless steel autoclave; the raw product was thereafter washed with hydrochloric acid to remove the by-product magnesium oxide, resulting in the bulk fibrous silicon/carbon composite sheet (Scheme S1d, ESI†); the thickness of the sheet depends on the filter paper used, which was *ca.* 40 μm in the current work.

Fig. 1 shows the electron micrographs of the silicon/carbon composite sheet prepared by using a silica/cellulose composite sheet with 20 cycles of silica gel film deposition. The FE-SEM images indicate that the silicon/carbon composite sheet is composed of randomly cross-linked microfibres which are assemblies of fine nanofibres (Fig. 1a and 1b), this structural feature is obviously inherited from the original filter paper. TEM micrograph of an individual silicon/carbon nanocomposite fibre clearly exhibits the nanocable structure of it, where thin silicon layer with a thickness about 20 nm is coated on the carbon nanofibre (Fig. 1c). A large number of fine silicon nanoparticles with sizes of *ca.* 4 nm are observed in the HR-TEM image of the composite fibre (Fig. 1d); and the diffraction rings 1–3 in the corresponding SAED pattern are indexed to (111), (101), and (100) diffractions of crystalline silicon (JCPDS# 47-1186), respectively, indicating the crystal nature of the silicon nanoparticles. It is observed that there is an ultrathin amorphous silicon oxide (SiO_x) layer with a thickness *ca.* 1 nm formed on the silicon surface of the composite fibre, which is due to exposure of the sample to air;[20] and this silicon oxide layer could serve as a buffer layer for the volume changes of the silicon nanocrystals upon charge/discharge cycles when the composite is employed as the anode of Li-ion batteries.[7a] The HR-TEM micrograph of a silicon nanocrystal immobilized on the composite fibre surface is shown in Fig. 1e, which displays clear crystal lattices with an interplanar distance of ~0.213 nm, matching with the (100) plane of silicon phase.

The silicon content of the silicon/carbon composites that derived from 20-cycles of silica gel film deposition was found to be 1.75% by weight obtained by energy dispersive X-ray (EDX) analyses. X-ray photoelectron spectrum (XPS) of the silicon/carbon composite sheet (Fig. S2a, ESI†) revealed a Si(2p) peak at 99.8 eV, indicating the presence of metallic silicon;[2a] and there were two other peaks located at 101.4 and 103.1 eV, which are indexed to silicon oxide (SiO_x, $x < 2$; and SiO_2) due to the oxidation of the silicon nanocrystals in air,[7a,20c] agreeing well with the TEM results shown above. Two C(1s) peaks were observed to be at 284.6 and 288.4 eV (Fig. S2b, ESI†), which are assigned to hydrocarbon and C–O–Si, respectively,[21] the latter one indicates the chemical interaction in-between the carbon nanofibres and the silicon nanocrystals. Although the formation of the silicon oxide would reduce the charge-discharge capacity and the Coulombic efficiency of the anodes at a certain extent, the silicon oxide layer is believed to enhance the adhesive force between silicon and carbon,[20c] and to accommodate the volume change of the silicon matter during the charge/discharge processes leading to enhanced stability of the anodes.[22] Both X-ray diffraction (XRD) patterns of the silica/carbon and silicon/carbon nanocomposite sheets (Fig. S3, ESI†) showed two broad diffraction peaks at $2\theta = 23°$ and 43°, which are indexed to the (002) and (100) planes of carbon, indicating the non-graphitized structure of the carbon nanofibres.[23] Diffraction peaks of the silicon component were not observed due to its relatively low content in the composite, and because that the ultra-small silicon nanocrystals are homogeneously distributed on the carbon nanofiber surfaces without aggregation as shown by the TEM observations.

The present silicon/carbon composite sheet is composed of carbon nanofibres with ultra-fine silicon nanocrystals immobilized uniformly and homogeneously on the surfaces of which, the bulk materials possesses the unique macro- to nano-scale hierarchical structures and morphologies that duplicated from the initial cellulose substance which was employed as both structural scaffold and carbon source. The three-dimensional porous network of the carbon nanofibres would facilitate the electron transfer, buffer the volume change and prevent the silicon nanoparticle aggregation during the charge/discharge processes. The high specific surface area of the composite resulted from the porous structure and the amorphous carbon nanofibres[19b] is expected to benefit the lithium-ion storage property of the anodes.

To evaluate the electrochemical properties of the nanofibrous silicon/carbon composite sheets fabricated, a square shaped piece of the sheet with size of ~6 × 6 mm^2 which weights *ca.* 1.3 mg was directly employed as the anode without adding any binding or conducting additive and as the current collector to make a standard CR2025 type coin cell with lithium foil as the counter electrode and Celgard 2300 as the separator; and the electrolyte used was 1.0 M $LiPF_6$ in ethylene carbonate (EC), dimethyl carbonate (DMC), and ethyl methyl carbonate (EMC) with a volume ration of 1:1:1. Fig. 2a shows the cyclic voltammetry (CV) curves of the silicon/carbon composite sheet derived from the as-deposited silica/cellulose composite sheet with 20 cycles of silica gel film deposition. In the first cathodic half-cycle (lithium ion insertion), a broad irreversible cathodic peak is shown at around 0.40 V due to the formation of the interface between the composite and the electrolyte; which is disappeared in the following cycles, indicating the formation of a stable solid electrolyte interface (SEI) film.[21,24] The cathodic peak at near to 0.10 V is ascribed to the formation of a series of lithium-silicon alloys (Li_xSi).[25] In the first anodic scan (lithium ion extraction), the broad anodic peaks occur at 0.2–0.6 V is corresponded to the phase transition between amorphous Li_xSi to amorphous silicon.[26] The electrode peaks were stable and no obvious differences was observed in the subsequent cycles, indicating the good reversible capacity and cycling performance.[24]

Fig. 2b displays the voltage profiles for the 1st, 2nd and 20th galvanostatic charge/discharge curves of such a cell in the voltage window of 0.01–3.0 V versus Li/Li^+ at a current density of 100 mA g^{-1}. In the first cycle, the potential plateau at *ca.* 0.1 V is due to the alloying process of silicon and lithium, and the other slope

at *ca.* 0.8 V is attributed to the SEI film formation;[25a] which disappeared in the following cycles, agreeing with the CV measurements. The first cycle discharge and charge capacities were 2.60 and 1.15 mAh cm^{-2}, respectively; and the Coulombic efficiency was 44.2%, the low value is caused by the formation of the SEI layer [27], and by the reduction of the SiO_x formed on the surface of silicon nanocrystals.[22] The charge and discharge profiles are similar from the second cycle, indicating the good cycling stability of the silicon/carbon composite sheet. The galvanostatic cycling performance of the free-standing silicon/carbon composite anode at a current density of 100 mA g^{-1} is shown in Fig. 2c, the reversible capacity is relatively constant with Coulombic efficiency of generally ~99% from the second cycle and onward, indicating the high stability of the silicon/carbon composite. The reversible capacity after 100 cycles is 1.04 mAh cm^{-2} (89% of the second cycle). Compared with silicon nanoparticles, better stable cycling performance is achieved for the silicon/carbon composite; while the slow and inconspicuous fade is due to the lost of electric contact between the silicon nanocrystals and the carbon fibres caused by the volume change during the charge/discharge processes. As a control study, the reversible capacities of the carbon sheet that obtained by carbonization of filter paper and the silica/carbon composite sheet (Scheme S1c, ESI†) were measured to be both *ca.* 0.75 mAh cm^{-2} after 100 cycles. Considering the low silicon content (1.75 wt%) in the silicon/carbon composite sheet, the contribution of the silicon nanocrystals to the improved reversible capacity is significant, and the current cycling areal capacity is better than those of the silicon nanowire network anode (~0.6 mAh cm^{-2})[2b] and the three-dimensional Ni/TiO_2 nanowire network anode.[28]

Fig. 2d presents the rate performance of the silicon/carbon composite anode at different current densities, with increasing the current density from 0.36 mA cm^{-2} (100 mA g^{-1}) to 3.60 mA cm^{-2} (1 A g^{-1}), the capacity gradually decreases; and the capacity reversibly recovers to the initial value once the current rate goes back to 0.36 mA cm^{-2} with Coulombic efficiencies of ~100%. The excellent cycling behaviour and the significant capacity retention of the silicon/carbon composite sheet is due to the unique porous three-dimensional cross-linked network structures of it, which facilitate the effective contact of the electrolyte and the silicon nanoparticles as well as the electron percolation against the low intrinsic electric conductivity of silicon, accommodate the dramatic volume change induced by the lithium insertion/extraction reactions, and enable the structural and interfacial stabilization of the silicon nanocrystals. Moreover, the carbon nanofibres prevent the agglomeration of the silicon nanocrystals, hence the electrical and morphological integrity of the self-supporting anode is effectively preserved.

The structural integrity of the free-standing silicon/carbon composite anode upon charge/discharge processes was confirmed by electron microscope examinations. The porous three dimensional network structure of the composite sheet was maintained after 50 cycles (Fig. S4a, ESI†), which contributes to the good capacity maintenance of the anode; and all the composite fibres were observed to be prelithiated, considering that the composite was directly employed as the anode without using of current collector, it can be inferred that the composite possesses good electrical conductivity. The surface of the silicon/carbon nanofibres become porous after cycling (Fig. S4b, ESI†), which is due to the repeated lithium alloying and dealloying processes that resulted in the expansion/contraction of the fibres, which is consistent with the previous reports in the cases of silicon nanowires.[2b,4a,25c,29] And the silicon component in the cycled composite was in amorphous state, since the original crystalline silicon turns into amorphous after the initial cycles.[30]

In summary, we have demonstrated a facile, effective and low-cost pathway for the fabrication of nanofibrous silicon/carbon composite sheet with hierarchical morphologies employing natural cellulose substance (*e.g.*, commercial filter paper) as structural scaffold and carbon source. The free-standing composite sheet was used as anodes for Li-ion batteries as both active material and current collector without adding of any binder or conducting additive; and due to the unique porous three dimensional network structures of which, it showed good areal capacity as well as improved cycling and rate performances. Although further works are needed to achieve better battery capacities, the current work sheds new light on the development of bio-inspired nanomaterials that offer prospect for future energy applications for a cleaner environment, which could be benefited from the naturally produced sophisticated structures that inherited by the artificial materials.

This work was supported by the National Natural Science Foundation of China (21173192).

Notes and references

1 (*a*) H. K. Liu, Z. P. Guo, J. Z. Wang and K. Konstantinov, *J. Mater. Chem.*, 2010, **20**, 10055–10057; (*b*) J. Cho, *J. Mater. Chem.*, 2010, **20**, 4009; (*c*) H. Wua and Y. Cui, *Nano Today*, 2012, **7**, 414.

2 (*a*) H. Kim, M. Seo, M.-H. Park and J. Cho, *Angew. Chem., Int. Ed.*, 2010, **49**, 2146; (*b*) L. Hu, H. Wu, S. S. Hong, L. Cui, J. R. McDonough, S. Bohy and Y. Cui, *Chem. Commun.*, 2011, **47**, 367.

3 (*a*) H. Kim, B. Han, J. Choo and J. Cho, *Angew. Chem., Int. Ed.*, 2008, **47**, 10151; (*b*) H. Jia, P. Gao, J. Yang, J. Wang, Y. Nuli and Z. Yang, *Adv. Energy Mater.*, 2011, **1**, 1036; (*c*) J. Zhu, C. Gladden, N. Liu, Y. Cui and X. Zhang, *Phys. Chem. Chem. Phys.*, 2013, **15**, 440. (*d*) Y. Yu, L. Gu, C. Zhu, S. Tsukimoto, P. A. van Aken and J. Maier, *Adv. Mater.*, 2010, **22**, 2247.

4 (*a*) N. Liu, L. Hu, M. T. McDowell, A. Jackson and Y. Cui, *ACS Nano*, 2011, **5**, 6487; (*b*) I. Ryu, J. W. Choi, Y. Cui and W. D. Nix, *J. Mech. Phys. Solids*, 2011, **59**, 1717.

5 (*a*) M.-H. Park, M. G. Kim, J. Joo, K. Kim, J. Kim, S. Ahn, Y. Cui and J. Cho, *Nano Lett.*, 2009, **9**, 3844; (*b*) H. Wu, G. Chan, J. W. Choi, I. Ryu, Y. Yao, M. T. McDowell, S. W. Lee, A. Jackson, Y. Yang, L. Hu and Y. Cui, *Nature Nanotech.*, 2012, **7**, 310. (*c*) J.-K. Yoo, J. Kim, Y. S. Jung and K. Kang, *Adv. Mater.*, 2012, **24**, 5452.

6 Y. Yao, M. T. McDowell, I. Ryu, H. Wu, N. Liu, L. Hu, W. D. Nix and Y. Cui, *Nano Lett.*, 2011, **11**, 2949.

7 (*a*) Y.-S. Hu, R. Demir-Cakan, M.-M. Titirici, J.-O. Müller, R. Schlögl, M. Antonietti and J. Maier, *Angew. Chem., Int. Ed.*, 2008, **47**, 1645; (*b*) P. Gao, J. Fu, J. Yang, R. Lv, J. Wang, Y. Nuli and X. Tang, *Phys. Chem. Chem. Phys.*, 2009, **11**, 11101.

8 (*a*) N. Liu, Z. Lu, J. Zhao, M. T. McDowell, H.-W. Lee, W. Zhao and Y. Cui, *Nature Nanotech.*, 2014, **9**, 187; (*b*) H. Wu, G. Zheng, N. Liu, T. J. Carney, Y. Yang and Y. Cui, *Nano Lett.*, 2012, **12**, 904.

9 (*a*) L. Ji and X. Zhang, *Carbon*, 2009, **47**, 3219; (*b*) Y. Li, B. Guo, L. Ji, Z. Lin, G. Xu, Y. Liang, S. Zhang, O. Toprakci, Y. Hu, M. Alcoutlabi and X. Zhang, *Carbon*, 2013, **51**, 185; (*c*) Y. Li, G. Xu, Y. Yao, L. Xue, S. Zhang, Y. Lu, O. Toprakci and X. Zhang, *J. Solid State Electrochem.*, 2013, **17**, 1393.

10 (*a*) G. K. Simon, B. Maruyama, M. F. Durstock, D. J. Burton and T. Goswami, *J. Power Sources*, 2010, **196**, 10254; (*b*) J. Y. Howe, D. J.

Burton, Y. Qi, H. M. Meyer III, M. Nazri, G. A. Nazri, A. C. Palmer and P. D. Lake, *J. Power Sources*, 2010, **221**, 455; (*c*) L.-F. Cui, Y. Yang, C.-M. Hsu and Y. Cui, *Nano Lett.*, 2009, **9**, 3370; (*d*) W. Wang and P. N. Kumta, *ACS Nano*, 2010, **4**, 2233; (*e*) Y. Fan, Q. Zhang, Q. Xiao, X. Wang and K. Huang, *Carbon*, 2013, **59**, 264.

11 Y. Zhu, W. Liu, X. Zhang, J. He, J. Chen, Y. Wang and T. Cao, *Langmuir*, 2013, **29**, 744.

12 L. Ji and X. Zhang, *Electrochem. Commun.*, 2009, **11**, 1146.

13 (*a*) L.-F. Cui, L. Hu, J. W. Choi and Y. Cui, *ACS Nano*, 2010, **4**, 3671; (*b*) J. W. Choi, L. Hu, L. Cui, J. R. McDonough and Y. Cui, *J. Power Sources*, 2010, **195**, 8311; (*c*) K.-S. Park, K.-M. Min, S.-D. Seo, G.-H. Lee, H.-W. Shim and D.-W. Kim, *Mater. Res. Bull.*, 2013, **48**, 1732.

14 (*a*) K. Evanoff, J. Benson, M. Schauer, I. Kovalenko, D. Lashmore, W. J. Ready and G. Yushin, *ACS Nano*, 2012, **6**, 9837; (*b*) Y. Liu, K. Huang, Y. Fan, Q. Zhang, F. Sun, T. Gao, Z. Wang and J. Zhong, *Electrochim. Acta*, 2013, **102**, 246; (*c*) A. M. Chockla, J. T. Harris, V. A. Akhavan, T. D. Bogart, V. C. Holmberg, C. Steinhagen, C. B. Mullins, K. J. Stevenson and B. A. Korgel, *J. Am. Chem. Soc.*, 2011, **133**, 20914; (*d*) B. Liu, X. Wang, H. Chen, Z. Wang, D. Chen, Y.-B. Cheng, C. Zhou and G. Shen, *Sci. Rep.*, 2013, **3**, 1622; DOI:10.1038/srep01622.

15 (*a*) S.-L. Chou, Y. Zhao, J.-Z. Wang, Z.-X. Chen, H.-K. Liu and S.-X. Dou, *J. Phys. Chem. C*, 2010, **114**, 15862; (*b*) L. Hua, N. Liu, M. Eskilsson, G. Zheng, J. McDonough, L. Wågberg and Y. Cui, *Nano Energy*, 2013, **2**, 138; (*c*) L. Yue, H. Zhong and L. Zhang, *Electrochim. Acta*, 2012, **76**, 326; (*d*) J. K. Lee, K. B. Smith, C. M. Hayner and H. H. Kung, *Chem. Commun.*, 2010, **46**, 2025; (*e*) L. Hu, H. Wu, Y. Gao, A. Cao, H. Li, J. McDough, X. Xie, M. Zhou and Y. Cui, *Adv. Energy Mater.*, 2011, **1**, 523.

16 B. Wang, X. Li, X. Zhang, B. Luo, M. Jin, M. Liang, S. A. Dayeh, S. T. Picraux and L. Zhi, *ACS Nano*, 2013, **7**, 1437.

17 (*a*) J. Li, H. Möhwald, Z. An and G. Lu, *Soft Matt.*, 2005, **1**, 259; (*b*) Q. He, Y. Cui and J. Li, *Chem. Soc. Rev.*, 2009, **38**, 2292; (*c*) Z. An, H. Möhwald and J. Li, *Biomacromolecules*,, 2006, **7**, 580; (*d*) Q. He, H. Möhwald and J. Li, *Macromol. Rapid Commun.*, 2009, **30**, 1538.

18 (*a*) J. Huang and T. Kunitake, *J. Am. Chem. Soc.*, 2003, **125**, 11834; (*b*) R. A. Caruso, *Angew. Chem., Int. Ed.*, 2004, **43**, 2746 ; (*c*) J. Huang, N. Matsunaga, K. Shimanoe, N. Yamazoe and T. Kunitake, *Chem. Mater.*, 2005, **17**, 3513.

19 (*a*) J. Huang, T. Kunitake and S. Onoue, *Chem. Commun.*, 2004, 1008; (*b*) X. Liu, Y. Gu and J. Huang, *Chem. Eur. J.,* 2010, **16**, 7730; (*c*) J. Zhao, Y. Gu and J. Huang, *Chem. Commun.*, 2011, **47**, 10551; (*d*) Y. Zhang, X. Liu and J. Huang, *ACS Appl. Mater. Interfaces*, 2011, **3**, 3272; (*e*) Y. Zhang and J. Huang, *J. Mater. Chem.*, 2011, **21**, 7161; (*f*) X. Liu, Y. Zhang, T. Wu and J. Huang, *Chem. Commun.*, 2012, **48**, 9992; (*g*) Y. Gu and J. Huang, *Chem. Eur. J.*, 2013, **19**, 10971.

20 (*a*) B.-S. Kim, T.-W. Koo, J.-H. Lee, D. S. Kim, Y. C. Jung, S. W. Hwang, B. L. Choi, E. K. Lee, J. M. Kim and D. Whang, *Nano Lett.*, 2009, **9**, 864; (*b*) M. S. Gudiksen, J. Wang and C. M. Lieber, *J. Phys. Chem. B*, 2001, **105**, 4062; (*c*) X. Xin, X. Zhou, F. Wang, X. Yao, X. Xu, Y. Zhu and Z. Liu, *J. Mater. Chem.*, 2012, **22**, 7724.

21 Y. Wang, S. Chou, J. H. Kim, H. Liu and S. Dou, *Electrochim. Acta,* 2013, **93**, 213.

22 L. Su, Z. Zhou and M. Ren, *Chem. Commun.,* 2010, **46**, 2590.

23 X. Shen, D. Mu, S. Chen, B. Xu, B. Wu and F. Wu, *J. Alloy Compd.,* 2013, **552**, 60.

24 Y. Yin, S. Xin, L. Wan, C. Li and Y. Guo, *J. Phys. Chem. C*, 2011, **115**, 14148.

25 (*a*) J. Deng, H. Ji, C. Yan, J. Zhang, W. Si, S. Baunack, S. Oswald, Y. Mei and O. G. Schmidt, *Angew. Chem., Int. Ed.*, 2013, **52**, 2326; (*b*) D. Chen, X. Mei, G. Ji, M. Lu, J. Xie, J. Lu and J. Lee, *Angew. Chem., Int. Ed.,* 2012, **51**, 2409; (*c*) C. K. Chan, H. L. Peng,G. Liu, K. McIlwrath, X. F. Zhang, R. A. Huggins and Y. Cui, *Nat. Nanotechnol.*, 2008, **3**, 31; (*d*) M. Green, E. Fielder, B. Scrosati, M. Wachtler and J. S. Moreno, *Electrochem. Solid-State Lett.*, 2003, **6**, A75.

26 (*a*) V. Baranchugov, E. Markevich, E. Pollak,G. Salitra and D. Aurbach, *Electrochem. Commun.*, 2007, **9**, 796; (*b*) J. R. Szczech and S. Jin, *Energy Environ. Sci.,* 2011, **4**, 56.

27 X. Chen, K. Gerasopoulos, J. Guo, A. Brown, C. Wang, R. Ghodssi and J. N. Culver, *ACS Nano,* 2010, **4**, 5366.

28 W. Wang, M. Tian, A. Abdulagatov, S. M. George, Y.-C. Lee and R. Yang, *Nano Lett.*, 2012, **12**, 655.

29 J. W. Choi, J. McDonough, S. Jeong, J. S. Yoo, C. K. Chan and Y. Cui, *Nano Lett.*, 2010, **10**, 1409.

30 (*a*) Y. M. Kang, S. M. Lee, S. J. Kim, G. J. Jeong, M. S. Sung, W. U. Choi and S. S. Kim, *Electrochem. Commun.*, 2007, **9**, 959; (*b*) J. Li and J. R. Dahn, *J. Electrochem. Soc.*, 2007, **154**, A156.

Figure Legends:

Fig. 1 The fibrous silicon/carbon nanocomposite sheet fabricated by employing cellulose filter paper as scaffold and carbon source. (a) Field emission scanning electron micrograph (FE-SEM), showing nanofibre assemblies. (b) A close view of the FE-SEM micrograph. (c) Transmission electron micrographs (TEM) of an individual silicon/carbon nanocomposite fibre. (d) High resolution TEM (HR-TEM) micrograph of the sample, the inset shows the corresponding selected-area electron diffraction (SAED) pattern. (e) HR-TEM image of the silicon layer of the nanocomposite fibre, showing silicon nanocrystal.

Fig. 2 Electrochemical performance of the hierarchical silicon/carbon nanocomposite sheet anode. (a) Cyclic voltammetry curves at a scan rate of 0.1 mV s^{-1} over the potential window of 0.01–3.0 V *vs.* Li/Li^{+}. (b) Galvanostatic charge/discharge profile for the 1st, 2nd and 20th cycle. (c) Areal charge/discharge capacity and Coulombic efficiency *vs.* cycle number at the current density of 100 mA g^{-1}, the first cycle is omitted for clarity. (d) Rate capabilities and Coulombic efficiency at various currents.

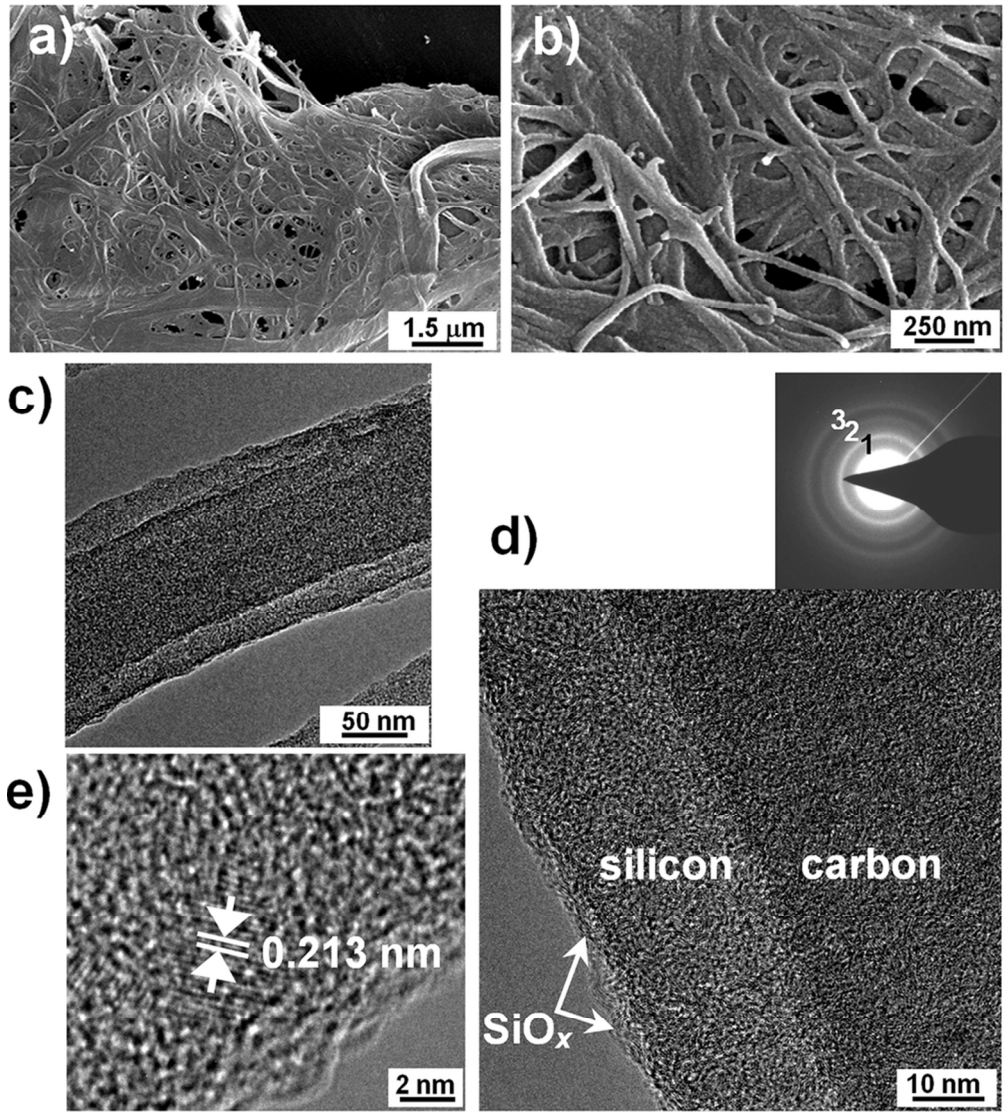

The fibrous silicon/carbon nanocomposite sheet fabricated by employing cellulose filter paper as scaffold and carbon source. (a) Field emission scanning electron micrograph (FE-SEM), showing nanofibre assemblies. (b) A close view of the FE-SEM micrograph. (c) Transmission electron micrographs (TEM) of an individual silicon/carbon nanocomposite fibre. (d) High resolution TEM (HR-TEM) micrograph of the sample, the inset shows the corresponding selected-area electron diffraction (SAED) pattern. (e) HR-TEM image of the silicon layer of the nanocomposite fibre, showing silicon nanocrystal.
42x47mm (600 x 600 DPI)

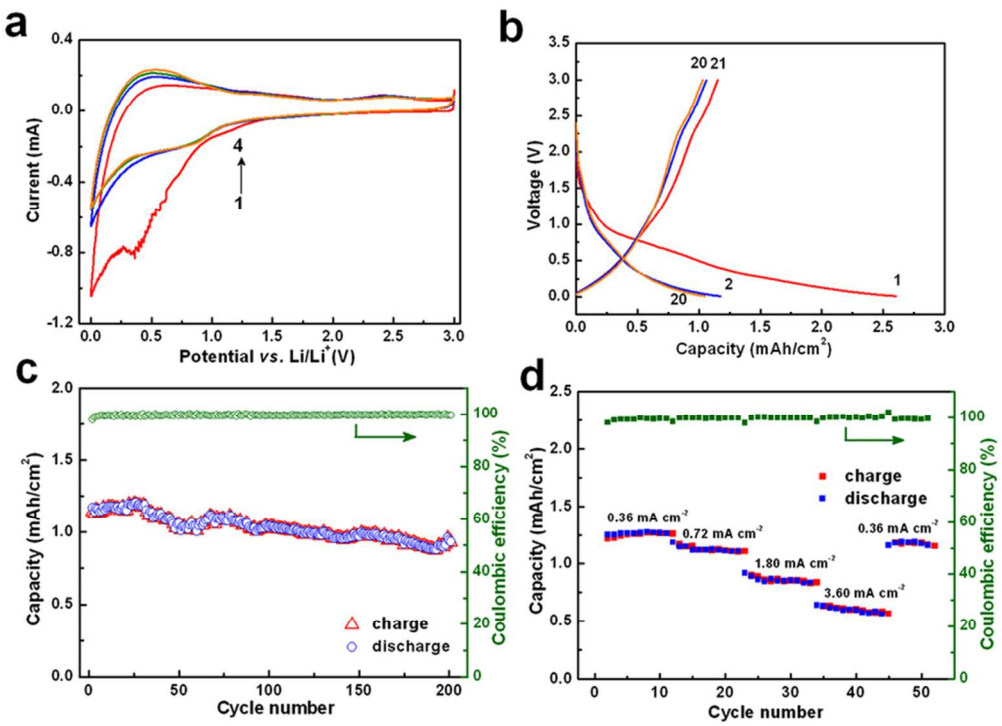

Electrochemical performance of the hierarchical silicon/carbon nanocomposite sheet anode. (a) Cyclic voltammetry curves at a scan rate of 0.1 mV s^{-1} over the potential window of 0.01–3.0 V *vs.* Li/Li^+. (b) Galvanostatic charge/discharge profile for the 1st, 2nd and 20th cycle. (c) Areal charge/discharge capacity and Coulombic efficiency *vs.* cycle number at the current density of 100 mA g^{-1}, the first cycle is omitted for clarity. (d) Rate capabilities and Coulombic efficiency at various currents.
36x26mm (600 x 600 DPI)

Nanofibrous silicon/carbon composite sheet derived from cellulose substance as free-standing lithium-ion battery anodes

Mengya Wang, Dongling Jia, Jiao Li and Jianguo Huang*

Department of Chemistry, Zhejiang University, Hangzhou, Zhejiang 310027, China

E-mail: jghuang@zju.edu.cn

Graphic Abstract Entry:

Nanofibrous silicon/carbon composite sheet derived from cellulose substance as free-standing lithium-ion battery anodes

Mengya Wang, Dongling Jia, Jiao Li and Jianguo Huang*

A bio-inspired nanofibrous Si/C composite sheet was fabricated and employed as self-supporting anode for Li-ion battery showing good electrochemical performances.